NOVEL WAVEFRONT SENSING STRATEGIES FOR STRONG ATMOSPHERIC TURBULENCE

OECD CONFERENCE CENTER, PARIS, FRANCE / 2–4 JANUARY 2016

Karin Stein [(1)], Szymon Gładysz [(1)], Andreas Zepp [(1)], Esdras Anzuola [(1)], Max Segel [(1)]

[(1)] Fraunhofer Institute of Optronics, System Technologies and Image Exploitation, Gutleuthausstr. 1
76275 Ettlingen, Germany, Email: karin.stein@iosb.fraunhofer.de

KEYWORDS: adaptive optics, atmospheric turbulence

ABSTRACT:

Atmospheric effects limit the performance of any electro-optical (EO) system. Tasks such as laser communication and delivery of directed energy are significantly affected by turbulence and refraction. A correction of atmospheric effects on the propagation of light can be done by adaptive optics (AO). Especially for astronomical applications, AO technology shows great promise for improving the performance of EO-systems. Nevertheless, challenging scenarios like a long horizontal path or strong scintillation lead to high failure rates of the EO systems. Adaptive optics methods and components developed for astronomical applications cannot fulfil these higher requirements. Unconventional wavefront sensors and sensing strategies are developed at Fraunhofer IOSB to provide alternatives for measuring the wavefront deformation of a laser beam and to improve the performance of laser communications and directed-energy weapons even in strong turbulence and/or horizontal-path propagation. In this paper we show the realization of the holographic wavefront sensor (HWFS) and we present results from two “wavefront-sensorless” approaches: stochastic parallel gradient descent (SPGD) and its modal version (M-SPGD).

1. ADAPTIVE OPTICS WITH AND WITHOUT A WAVEFRONT SENSOR

Adaptive optics (AO), a technology which encompasses a variety of electro-optical systems aiming at measurement and correction of optical deformations in real time, has found many applications in today’s World: astronomy, in vivo imaging of human retina, vision correction, laser machining, remote sensing, tracking and high-resolution imaging of satellites, missile defence, communications and even entertainment (in DVD players), to name just a few. The systems and methods of AO are crossing over to consumer market because of constant decline in prices of deformable mirrors and speed-up of computations available on a personal computer.

1.1. Holographic wavefront sensor

A classic AO system consists of three elements: a wavefront sensor, a deformable mirror and a wavefront reconstruction algorithm/computer. Wavefront sensor, as the name suggests, is tasked with measuring the form of an incoming optical wavefront. This wavefront when exiting a target or light-source is often almost flat but it will immediately get perturbed by atmospheric turbulence when the target is within Earth’s atmosphere. There, tiny differences in air temperature will lead to differences in index of refraction across the wavefront. Warmer pockets of air will advance the wavefront, while colder ones will cause parts of it to lag behind. This will lead to a wavefront which is spatially and temporally varying. Wavefront sensor must reliably measure these aberrations. Reconstruction and control computer will then process wavefront information into a form that can be sent to a deformable mirror which will subsequently apply a correction to the “next” incoming wavefront, and so on, in a closed-loop system.

The well-established Shack-Hartmann wavefront sensor (SHS) is a workhorse solution in astronomical AO [1]. However, two fundamental characteristics handicap the application of this sensor to more challenging scenarios like laser propagation over long horizontal paths within extended-volume turbulence, which produce scintillation and branch points in the wavefronts. Firstly, due to the procedure of wavefront reconstruction, the bandwidth of SHS is limited. This has consequences for deploying SHS-based AO systems on moving platforms and/or for satellite tracking. Secondly, SHS is highly sensitive to scintillation effects. Obscurations or saturations of parts of the sensor’s pupil can lead to significant failure rate of the wavefront reconstruction process [2].

The weaknesses of the SHS seem to be the strengths of the so-called holographic wavefront sensor (HWFS) [3-5]. This sensor type consists of

two main components: a holographic diffractive optical element (DOE) and a small detector array. By illuminating the DOE with the beam of interest, it generates for each wavefront aberration (e.g., for each Zernike mode) two spots at predefined locations on the detector array (Fig. 1). The amplitude of each aberration can be determined from the normalized intensity difference of both spots. Hence, the modal decomposition of the wavefront into its components is a diffraction process and is carried out at the speed of light. There is no need for time-consuming matrix-vector multiplications inherent to SHS-based AO systems. Besides the potentially exceptional bandwidth capabilities of HWFS, the operational principle of the sensor is insensitive to partial pupil obscurations. We have tested obscurations up to 33% of the aperture size [6, 7]. These characteristic features make HWFS an ideal candidate for sensing atmospheric effects on laser propagation.

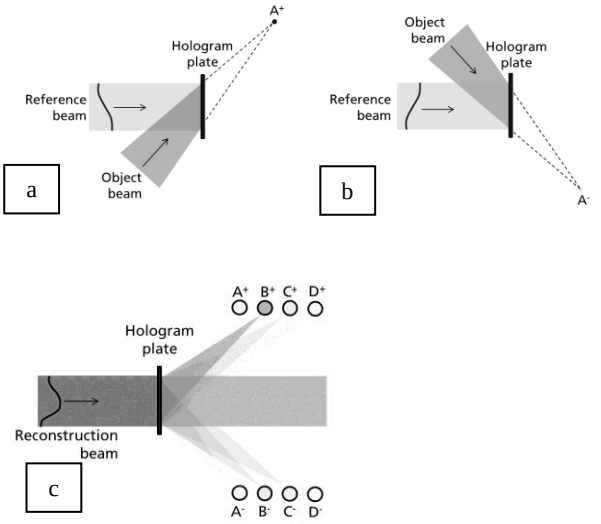

Figure 1. (a) Recording of a hologram with the positive amplitude of one chosen Zernike mode. (b) Recording with the negative amplitude of the same mode. The multiplex of both recordings is the core of HWFS for the measurement of one aberration type. (c) The hologram is encoded for the simultaneous measurement of four different Zernike modes (A, B, C, and D). If it is illuminated with a reconstruction beam, light is diffracted in all spots. The intensity difference of the matching spots gives information about the amplitude of a particular Zernike mode. In this example, only the mode B is present in the wavefront.

1.2. Blind wavefront measurement

In scenarios where wavefront measurement is either impossible, because of e.g. very high turbulence, or not necessary, e.g. in medicine where optical aberrations introduced by human body into the imaging equipment are static or slowly-evolving, the concept of "wavefront-sensorless" AO has become established [8]. Here, use is made of "smart" algorithms which "guess" various combinations of optical deformations until an improvement in image or laser beam quality is observed. Naturally, when applied to strong atmospheric turbulence the methods must be exceptionally fast in their convergence rate. The most famous method, the stochastic parallel gradient descent (SPGD) [9], is inherently "blind", i.e. it does not make any assumptions about the nature of the aberrations and the propagation formalism through an optical system.

In order to improve the convergence rate of SPGD the modal version of the algorithm, M-SPGD, was proposed [10,11]. In SPGD, one perturbs randomly the actuators on the deformable mirror and the image or beam quality metric is checked for improvement. This can become a highly-dimensional problem for modern deformable mirrors with many actuators. To reduce the number of degrees of freedom one can project the actuator space onto an orthogonal modal basis, e.g. Zernike polynomials and perturb these instead of actuators. Additional advantage of this approach is that one can include known turbulence statistics into the algorithm e.g. by optimizing gain of the algorithm for each mode (it is well known that low-order modes such as tip, tilt and defocus have more influence on image/beam quality than the higher-order modes).

2. IMPLEMENTATIONS

2.1. Holographic wavefront sensor

Core of the HWFS is a holographic diffraction grating. The holographic principle enables the storage and reconstruction of the full three-dimensional information pertaining to an object. For that purpose, a reference beam is superimposed in the plane of the hologram plate with light coming from the object. After the chemical post-processing of the plate, the fringes are stored as phase grating. By illuminating this grating with a playback beam corresponding to the reference beam, the light is diffracted into the real image of the object. This optical reconstruction of the object highly depends on the wavefront of the playback beam. If the playback wave does not match the phase-conjugated reference beam, the real image is generated with aberrations. The functioning principle of the holographic wavefront sensor is based on this effect: The intensity of an optically reconstructed object point is a measure for the aberrations in the beam.

The implementation of HWFS for a single wavefront aberration is shown in Fig. 1 (top panels). Two holograms are recorded one after another. The object beams are symmetrically-arranged converging beams forming foci behind the hologram plate at the positions denoted A^+ and A^-. The reference beams are collimated beams which have anti-conjugated wavefronts corresponding to specific anti-conjugated Zernike modes. For the first hologram the amplitude of the chosen aberration is $+a$, where a is the maximum

amplitude of the chosen mode that the HWFS will be able to measure. For the second hologram the amplitude is *-a*.
After the exposure and chemical processing of the hologram, it can be used as diffraction grating for the laser beam of interest. The incoming light is diffracted into positions A^+ and A^-. It has been calculated that the normalized difference of intensities $(I_{A+} - I_{A-}) / (I_{A+} + I_{A-})$, integrated over a small area on the detector, is proportional, within a certain range, to the amount of the measured aberration mode contained in the input wavefront. Measuring the diffracted intensities at the spot positions A^+ and A^- gives information about the amplitude of the aberration. The sensor can be expanded for measuring more (e.g. Zernike) modes by multiplexing more holograms in the hologram plate (two for each mode, see bottom panel in Fig. 1).
Our implementation of HWFS is discussed in detail in [12]. In Fig. 2 the setup is illustrated schematically. As corrector in the AO system we use DM-52 from Alpao with 52 actuators.

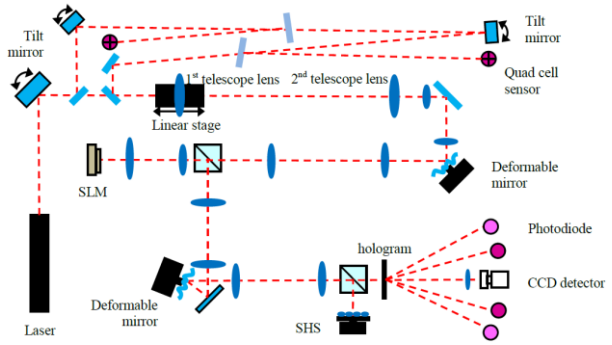

Figure 2. Experimental setup for evaluating the performance of a HWFS is shown schematically: A fast steering mirror (tilt mirror), an adaptable telescope with a movable lens, a deformable mirror (DM) as well as a spatial light modulator (SLM) can be used as aberrators. A second DM and two tilt mirrors form the correctors of the setup. As detectors a HWFS (consisting of hologram and photodiodes), a Shack-Hartmann sensor (SHS) and a CCD camera are implemented.

We now show a couple of results obtained with the HWFS coded for defocus. Firstly, constant aberration amplitude has been applied to the incoming beam. Different obscuration masks have been introduced to change the intensity distribution of the beam corresponding to scintillation effects. For each mask the HWFS has been used to measure the present aberration. The standard deviation of 1000 measurement with each mask is displayed in Fig. 3 (right panel). The fluctuation of the measured amplitude did not increase due to the partial obscuration of the beam. The experiments show that the presence of static obscurations has no significant influence on the performance of the holographic wavefront sensor.

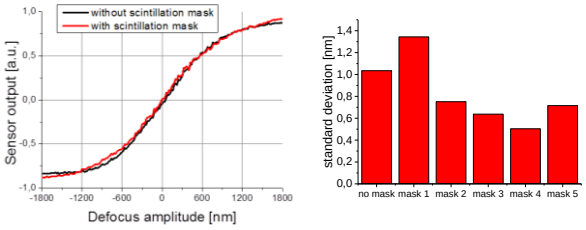

Figure 3. Left: Characteristic curve of a HWFS coded for defocus with and without a present intensity mask. Right: Standard deviation of defocus measurements of a static aberration for different intensity masks.

After the sensor calibration, a closed-loop AO system was implemented. The adaptive telescope acted as aberrator, the Alpao deformable mirror as corrector. The light was split into two parts: The zero order was transmitted by the hologram and used to gauge the quality of the beam imaged on a CCD camera. The first order was diffracted into two spots for each Zernike mode, detected by photodiodes. The photodiode signal is transmitted to a computer via a BNC-USB interface (USB-6251 BNC from National instruments). With Labview software the HWFS signal is transformed to a control signal for the deformable mirror.
With the described combination of photodiodes, interface and data processing with Labview a maximum bandwidth for measuring one Zernike mode of 11 kHz has been achieved. This was determined by triggering the data acquisition with increasing frequencies provided by an external frequency generator. The loop bandwidth of data acquisition and processing was measured in Labview. Expanding the system to 6 Zernike modes decreased the bandwidth to 2.5 kHz.
The decomposition of the incoming wavefront into the Zernike modes is a diffraction process and done at the speed of light. The photocurrent of the photodiodes is terminated with a 50 kΩ resistor. Thus the bandwidth of the readout amounts to approximately 230 kHz. Limiting factor is the computer-based signal processing. Optimization of hard- and software will increase the attainable bandwidth noticeably.
Fig. 4 (top panel) combines the first 10 correction steps in one graph. After three steps the normalized maximum intensity of the beam is enhanced from about 10% to more than 80%. With regards to the possible applications of the HWFS, the correction of the wavefront error should lead to increased power-in-the-bucket or an enhanced fiber-coupling efficiency. To consider this, a fixed circular region of interest (ROI) was defined. The size of this ROI corresponds to the waist of the unaberrated beam in the focal plane. The integrated intensity in this ROI should be maximized during the correction process.
In the middle panel in Fig. 4 the integrated intensity (normalized to the integrated intensity of the unaberrated beam) is shown vs. iteration number for different initial aberration amplitudes. The solid

line indicates the mean of the measurements. After three steps the mean is enhanced to over 90%.
In the bottom panel of Fig. 4 the residual absolute value of the aberration amplitude (in this example defocus) is presented. The mean amplitude is reduced to below 15 nm after four correction steps.

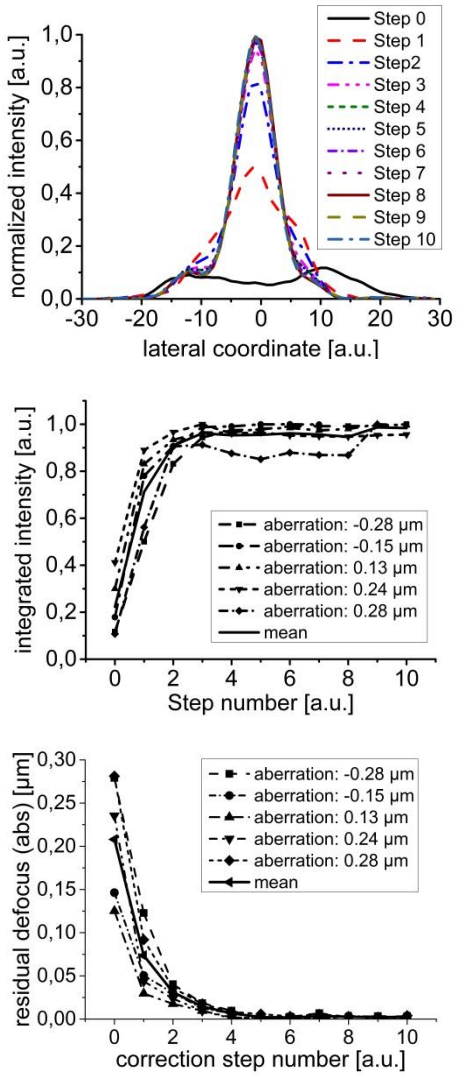

Figure 4. Left: Cross-sections of the intensity distributions of the laser beam in the focal plane after 1-10 correction steps. Middle: Dependency of integrated intensity (diameter of integration area equals the beam waist) on the number of correction steps for different initial aberrations. Right: Dependency of residual defocus (absolute value) on the number of correction steps for different initial aberrations.

To summarize, we have shown that the holographic wavefront sensor is capable of measuring optical aberrations, within its dynamic range, and driving an AO system.

2.2. Modal stochastic parallel gradient descent

Traditional SPGD algorithm can be written in the following way. Firstly, at each iteration *m* random negative and positive perturbations $\pm\gamma_n^m\,\delta u$, where γ_n^m is a random sign vector and δu is the perturbation factor, are applied to the actuators u_n:

$$u_n^{m+} = u_n^m + \gamma_n^m\,\delta u \quad (1)$$

$$u_n^{m-} = u_n^m - \gamma_n^m\,\delta u \quad (2)$$

Subsequently, change in the quality metric, in our case the Strehl ratio, is measured:

$$\delta J^m = J(u_n^{m+}) - J(u_n^{m-}) \quad (3)$$

Then, update of the control signal multiplied by the gain *G*, follows as:

$$u_n^{m+1} = u_n^m + G\,\delta J^m\,\gamma_n^m\,\delta u \quad (4)$$

Algorithm always converges, however speed of convergence and correction gain depend on choice of the parameters *G* and perturbation factor δu.
In our implementation the positive and negative perturbations from Eq. 1 are applied to Zernike modes and not to actuators. Therefore, at each iteration, current vector of Zernike coefficients has to be projected onto actuator voltages in order to drive the DM. This causes an additional overhead but the convergence rate of M-SPGD is still significantly increased as compared to traditional SPGD.
The setup for testing M-SPGD is shown schematically in Fig. 5. Photograph of the bread-board demonstrator is shown in Fig. 6.

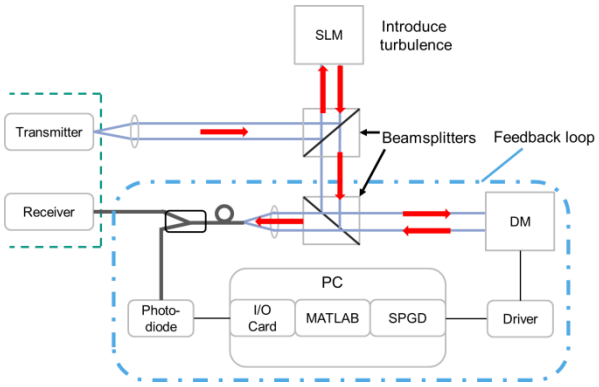

Figure 5. Diagram showing the setup for testing M-SPGD algorithm for the laser communications applications. Simulated turbulence (a phase screen from the Fourier-based method) is introduced into the setup through the spatial light modulator (SLM).

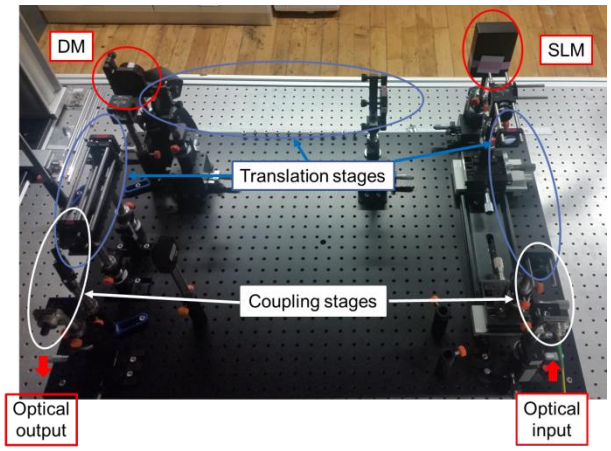

Figure 6. Actual optical system from Fig. 5.

In our initial results we have indeed demonstrated faster convergence rate of the M-SPGD algorithm as compared to the traditional SPGD. In Fig. 7 the evolution of the Strehl ratio vs. iteration number is shown for both approaches. Although classic SPGD achieves higher Strehl ratios, it converges slower than M-SPGD. In the interesting regime of less than 100 iterations M-SPGD performs better than SPGD.

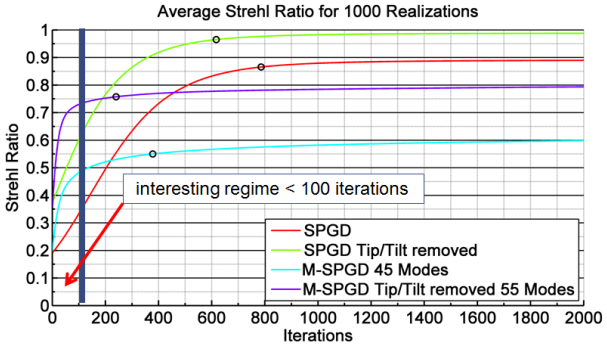

Figure 7. Illustration of convergence of SPGD and M-SPGD algorithms. Black circles denote points on the curves where the quality metric, here the Strehl ratio, starts to change by less than 10^{-4}. The blue vertical line denotes the region of less than 100 iterations which for practical reasons is the most interesting.

3. CONCLUSIONS

The holographic wavefront sensor is a promising alternative to the Shack-Hartmann device. The bandwidth restriction and the sensitivity to scintillation limit the use of the latter under challenging conditions like laser communications or directed energy. We were able to perform measurements with an analogue HWFS at a bandwidth of 11 kHz for a single aberration. Due to data acquisition and processing hardware the bandwidth is reduced when measuring more aberrations simultaneously. For two modes we achieved a bandwidth of 6.5 kHz and six modes were measured with 2.5 kHz. An optimization of the hardware will eliminate the dependency of the measurement speed on the number of aberrations.

Furthermore we operated the HWFS in a closed-loop AO system and achieved a bandwidth of 600 Hz. Limiting factor for the bandwidth is not the HWFS but the control computer and the bandwidth of the employed deformable mirror. In future we are planning to use a faster mirror controlled by a FPGA board to reach maximum loop bandwidths.
In principle, it is possible to avoid using a wavefront sensor in an AO system altogether. In the wavefront-sensorless approach we have tested two algorithms: SPGD and its modal version, M-SPGD. We have found faster convergence rate of the latter. More work on this approach is needed. In particular, we will research possible gains in convergence rate of M-SPGD with the inclusion of extra physical knowledge about turbulence.

4. ACKNOWLEDGMENTS

This research is part of the project ATLIMIS (Atmospheric Limitations of Military Systems, No. E/UR1M/9A265/AF170), commissioned and sponsored by the WTD91 (Technical Centre of Weapons and Ammunition) of the German Armed Forces.

5. REFERENCES

[1] R. K. Tyson, in 'Principles of Adaptive Optics – 3rd edition', (CRC Press, Boca Raton, 2011).

[2] G. Marchi and C. Scheifling, Proc. SPIE 8520, 85200C-1–15 (2012).

[3] M. A. A. Neil, M. J. Booth and T. Wilson, J. Opt. Soc. Am. A 17, 1098-1107 (2000).

[4] M. A. A. Neil, M. J. Booth and T. Wilson, Opt. Lett. 25, 1083-1085 (2000).

[5] G. P. Andersen, L. Dussan, F. Ghebremichael and K. Chen, Opt. Eng. 48, 085801 (2009).

[6] A. Zepp, Proc. SPIE 8535, 85350I (2012).

[7] A. Zepp, Proc. SPIE 8890, 88901F-1 (2013).

[8] R. A. Muller and A. Buffington, J Opt. Soc. Am.67, 1200-1210 (1974).

[9] M. A. Vorontsov, G. W. Carhart, and J. C. Ricklin, Opt. Lett. 22, 907-909 (1997).

[10] Q. Fu, J.-U. Pott, F. Shen and C. Rao, Opt. Comm. 310, 138-149 (2014).

[11] G. Xie, et al., Opt. Lett. 40, 1197-1200 (2015).

[12] A. Zepp, S. Gladysz, R. Barros, W. Osten, K. Stein, Proc. SPIE 9614, (2015).